

# Shortcuts for Adiabatic and Variational Algorithms in Molecular Simulation

Julían Ferreiro-Vélez,<sup>1,2,3,\*</sup> Iñaki Iriarte-Zendoia,<sup>1,3</sup> Yue Ban,<sup>4</sup> and Xi Chen<sup>5,†</sup>

<sup>1</sup>*Department of Physical Chemistry, University of the Basque Country UPV/EHU, Apartado 644, 48080 Bilbao, Spain*

<sup>2</sup>*TECNALIA, Basque Research and Technology Alliance (BRTA), 48160 Derio, Spain*

<sup>3</sup>*EHU Quantum Center, University of the Basque Country UPV/EHU, 48940 Leioa, Spain*

<sup>4</sup>*Departamento de Física, Universidad Carlos III de Madrid, Avda. de la Universidad 30, 28911 Leganés, Spain*

<sup>5</sup>*Instituto de Ciencia de Materiales de Madrid (CSIC), Cantoblanco, E-28049 Madrid, Spain*

(Dated: July 31, 2024)

Quantum algorithms are prominent in the pursuit of achieving quantum advantage in various computational tasks. However, addressing challenges, such as limited qubit coherence and high error rate in near-term devices, requires extensive efforts. In this paper, we present a substantial stride in quantum chemistry by integrating shortcuts-to-adiabaticity techniques into adiabatic and variational algorithms for calculating the molecular ground state. Our approach includes the counter-diabatic driving that accelerates adiabatic evolution by mitigating adiabatic errors. Additionally, we introduce the counter-diabatic terms as the adiabatic gauge ansatz for the variational quantum eigensolver, which exhibits favorable convergence properties with a fewer number of parameters, thereby reducing the circuit depth. Our approach achieves comparable accuracy to other established ansatzes, while enhancing the potential for applications in material science, drug discovery, and molecular simulations.

## I. INTRODUCTION

In the last decades, quantum technologies have undergone significant advances in the engineering and manipulation of quantum systems [1]. These advancements have led to the emergence of new quantum-based protocols, exploiting properties of the quantum mechanics for computing [2], communication [3, 4] or sensing [5, 6]. Since the inception of quantum computing in the 1980s, simulation of quantum many-body systems has been considered a litmus test in the field [7]. Quantum computers strive to efficiently simulate these systems by leveraging quantum properties, such as entanglement and the exponential scaling of Hilbert space, thereby overcoming the classical computational limitations.

In the realm of quantum simulation, modeling chemical systems stands out as one of the most promising applications of quantum computing in the near future. Quantum chemistry focuses on simulating the properties and dynamics of molecules and materials by applying the principles of quantum mechanics [8, 9]. Classical approaches to chemical simulation have yielded precise and successful results in material research. However, the high cost of simulating quantum systems with classical computers limits their application to large correlated systems. Conversely, quantum platforms can naturally simulate these systems, benefitting from the efficient encoding and the native simulation of quantum systems. Various algorithms have been proposed in the field of quantum simulation including: (i) Quantum Phase Estimation (QPE) [10]. This method utilizes the Quantum Fourier transform to compute the eigenstates and energies of the Hamiltonian [11, 12]. (ii) Adiabatic quantum computing (AQC) [13, 14]. AQC employs slow Hamiltonian evolution schedules to translate the system's ground state from an easily prepared state to the final problem ground state. (iii) Variational Quantum Eigen-

solver (VQE) [15, 16]. VQE is a hybrid quantum-classical algorithm that leverages classical optimization subroutines and parameterized quantum circuits to find the ground state of the Hamiltonian.

Despite significant progress in quantum system engineering, current quantum devices face challenges in fabricating large-scale systems protected against errors and noise [17]. These limitations constrain algorithm design, hindering the implementation of fault-tolerant algorithms like QPE, Shor's algorithm [18], and Grover's algorithm [19]. In contrast, adiabatic and variational algorithms are tailored for quantum hardware in noisy intermediate-scale quantum (NISQ) era, making them suitable for practical quantum computing applications [20]. Adiabatic algorithms for molecule simulation have received little attention, with relatively few studies conducted in this area [21, 22], primarily due to the resource-intensive nature of implementing time-dependent molecule Hamiltonians with numerous gates. Although recent studies have improved the scalability of these algorithms [23, 24], further exploration is needed to extend adiabatic computations to larger molecules. Meanwhile, the VQE algorithm has been extensively studied in quantum chemistry, demonstrating good performance in smaller molecule sizes [25–28]. However, its heuristic nature requires careful circuit design to effectively scale to larger molecules. Designing compact ansatzes is essential to overcome challenges such as decoherence, noise, and barren plateaus induced by circuit depth [29–31]. Until now, several notable approaches have been proposed for designing ansatzes, including QCC [32], UCCSD [33], HEA [34], ADAPT-VQE [35], and their variants. These ansatzes can be categorized based on their origins and design principles: hardware-efficient ansatzes are crafted for ease of its preparation within current quantum hardware [36, 37]; chemically inspired ansatzes are built on established classical quantum chemistry ansatzes [33, 38]; and Hamiltonian variational ansatzes leverage information from the system Hamiltonian for their construction [39].

Motivated by the current state of quantum chemistry, we

\* [julian.ferreiro@tecnalia.com](mailto:julian.ferreiro@tecnalia.com)

† [xi.chen@csic.es](mailto:xi.chen@csic.es)

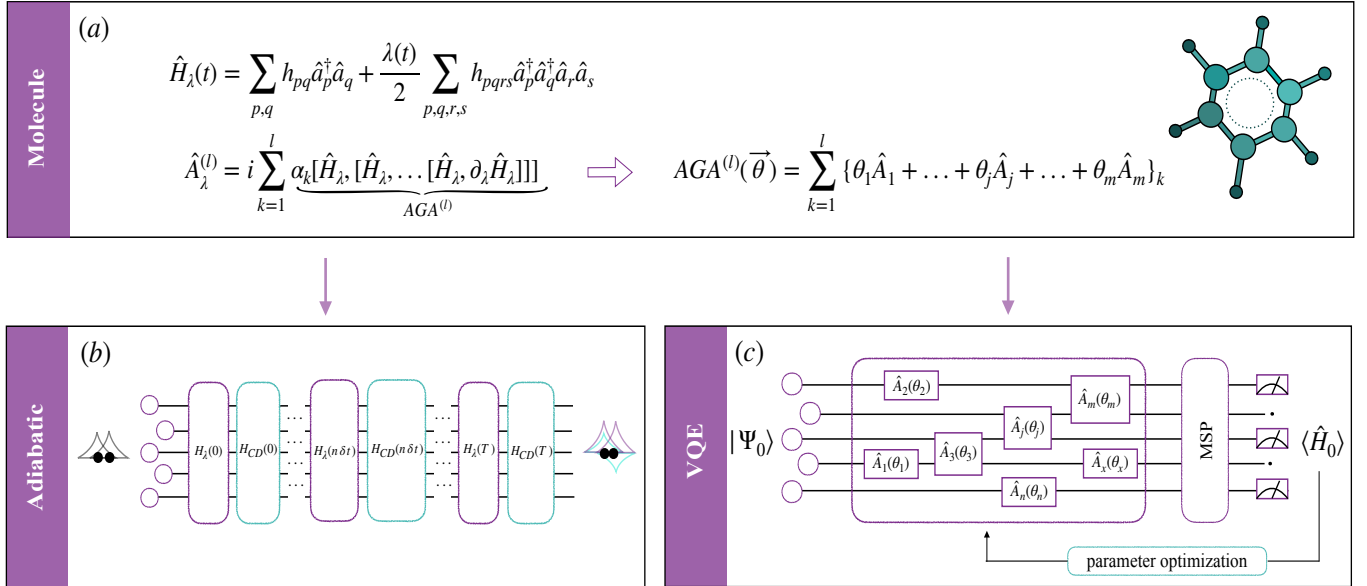


FIG. 1. Schematic representation of the CD protocol, rooted in shortcuts to adiabaticity, utilized for finding the ground state of the molecule. (a) The molecule block presents the Hamiltonian used in AQC for calculating the ground-state energy of molecules, along with the corresponding nested commutator technique. Additionally, the approximate CD term is outlined for defining the *adiabatic gauge ansatz* (AGA). (b) The adiabatic block depicts the preparation of the molecule’s ground state, starting from the free electron-electron system and transitioning to the full-interacting system. (c) Finally, the VQE block represents the variational circuit for the ground-state search, presenting the structure of the AGA-based circuit, the measure state preparation block (MSP) which prepares the circuit state for measuring the Hamiltonian expected value and the classical optimization subroutine.

aim to explore shortcuts to adiabaticity (STA) techniques [40] to enhance the performance of AQC and VQE in preparing the ground state of molecules. A prominent STA technique is CD driving [41, 42], which employs an auxiliary interacting Hamiltonian to guide the system along the adiabatic eigenstate trajectory with shorter time [43–46]. Despite being an exact technique, CD requires the solution of the full Schrödinger equation, which is often unavailable in many-body systems. In recent years, to address this problem, various local or approximate CD methods have been developed using techniques, such as the variational principle [47, 48], neural networks [49, 50], and counter-diabatic optimized local driving (COLD) [51]. These approaches are applicable to control complex many-body spin systems, facilitating improved digitized adiabatic quantum computing (DAQC) [52–55], optimizing the annealing schedule to expedite the adiabatic process [56–59], and enhancing quantum optimization algorithms [60–62] with reduced computational resource and shallow circuit.

In this work, we first apply approximate CD driving calculated from nested commutators [47, 48] to accelerate adiabatic algorithms and later extend this concept to design ansatzes in VQE for quantum chemistry. A schematic diagram illustrating our main strategy is shown in Fig. 1. In adiabatic algorithms, CD driving accelerates the adiabatic evolution, enabling faster convergence to the ground state of the molecule’s Hamiltonian with shallow circuits, see Fig. 1(b). This method is particularly effective in reducing the computational resources required for large-scale simulations.

Moreover, within VQE framework, we design a CD-inspired ansatz, termed as *adiabatic gauge ansatz* (AGA), as shown in Fig. 1(c), which leverages the evolution information encapsulated in the CD Hamiltonian to construct compact and expressive circuits for molecular simulations. This approach significantly enhances the efficiency and scalability of the algorithm [50, 63], enabling better performance with fewer parameters, making it particularly well-suited for NISQ device implementation. In contrast to adiabatic algorithms with CD driving, by using AGA in the VQE algorithm, the complex optimization of the CD terms is intrinsically addressed within the classical optimization loop, thereby streamlining the overall computational process.

The remainder of this article is organized as follows: Sec. II introduces the Hamiltonian and model of electronic molecular systems, along with the formalism of CD within the STA framework. Sec. III demonstrates the application of CD driving to enhance adiabatic algorithms for calculating molecular ground states. Sec. IV describes the CD-inspired ansatz in VQE and benchmarks its performance against alternative approaches. Finally, Sec. V provides conclusion and outlook for future research.

## II. MODEL, HAMILTONIAN AND CD METHOD

Here we focus on the efficient preparation of electronic orbital states on quantum computers. Starting from the Born-Oppenheimer approximation, we define the effective

electronic Hamiltonian by only considering the electronic-dependent terms in the Hamiltonian:

$$\hat{H}_0 = - \sum_{i=1}^N \frac{1}{2} \nabla_i^2 - \sum_{i=1}^N \sum_{A=1}^M \frac{Z_A}{r_{iA}} + \sum_{i=1}^N \sum_{j>i}^N \frac{1}{r_{ij}}, \quad (1)$$

where  $\nabla_i^2$  is the electron kinetic term, the second term denotes the nuclei-electron Coulomb attraction, and the last term accounts for the electronic repulsion. We translate the electronic molecular Hamiltonian (1) into the second-order quantization formalism, expressing the Hamiltonian as a sum of fermionic creation (annihilation) operators  $\hat{a}_p^\dagger$  ( $\hat{a}_p$ ) weighted by the one (two)-body coefficients  $h_{pq}$  ( $h_{pqrs}$ ) [64, 65], namely,

$$\hat{H}_0 = \sum_{p,q} h_{pq} \hat{a}_p^\dagger \hat{a}_q + \sum_{p,q,r,s} h_{pqrs} \hat{a}_p^\dagger \hat{a}_q^\dagger \hat{a}_r \hat{a}_s. \quad (2)$$

The new Hamiltonian represents the molecule wave function as a weighted sum of electronic orbitals, where the one-body and two-body coefficients  $h_{pq}$ ,  $h_{pqrs}$  encapsulate the molecule spin and spatial information, e.g., depending on the bond distance  $\vec{R}_b$  [15, 25, 27]. This representation can be directly mapped into the qubit notation by rewriting the creation and annihilation operators as a combination of Pauli matrix tensor products  $\{\hat{a}_p^\dagger, \hat{a}_p\} \rightarrow \{\hat{X}, \hat{Y}, \hat{Z}\}$ , enabling its implementation on a quantum computer. Examples of such mappings include the Jordan-Wigner (JW) transformation [66], the Bravyi-Kitaev (BK) transformation [67, 68], and the parity transformation [68], among others. For instance, the JW transformation maps the fermionic operators to qubit operators as follows:

$$\hat{a}_p \rightarrow \frac{1}{2} (\hat{X}_p + i\hat{Y}_p) \hat{Z}_1 \dots \hat{Z}_{p-1}, \quad (3)$$

where  $\hat{a}_p$  is the fermionic annihilation operator, and  $\hat{X}_p$ ,  $\hat{Y}_p$ , and  $\hat{Z}_p$  are the Pauli operators acting on the qubit corresponding to the  $p$ -th orbital. While the JW transformation is a well-established method, more sophisticated mappings can be advantageous for certain systems. In this work, we focus on the BK transformation, as detailed in [67], which maintains system locality and reduces the number of required qubit operations.

The computational resources required to find the ground state of the molecular Hamiltonian (2) scale exponentially with the number of electrons in the system. To address this challenge, we shall employ the extended Hartree-Fock (HF) approximation to compute the ground state from the electronic-repulsion-free Hamiltonian, and gradually increase the non-local electron repulsion. By following this approach, the molecular Hamiltonian can be reformulated into the adiabatic formalism as follows:

$$\hat{H}_\lambda(t) = \sum_{p,q} h_{pq} \hat{a}_p^\dagger \hat{a}_q + \frac{\lambda(t)}{2} \sum_{p,q,r,s} h_{pqrs} \hat{a}_p^\dagger \hat{a}_q^\dagger \hat{a}_r \hat{a}_s. \quad (4)$$

where  $\lambda(t)$  is the adiabatic schedule function for the electron-electron repulsion. Without loss of generality, we choose  $\lambda(t) = \sin^2(\pi t/2T)$ , which guarantees the initial and final boundary conditions:  $\hat{H}_\lambda(0) = \hat{H}(0)$  and  $\hat{H}_\lambda(T) = \hat{H}(T)$ , with

$T$  being the total operation time. Starting from the adiabatic molecule Hamiltonian (4), we compute the CD Hamiltonian for the molecular system. Employing the process evolution information contained in the CD-Hamiltonian for assisting the adiabatic state preparation in the AQC and VQE quantum algorithm, see Fig. 1.

The CD Hamiltonian introduces an additional term to the original time-dependent Hamiltonian  $\hat{H}_\lambda(t)$ , in order to mitigate non-adiabatic transitions induced by violations of the adiabatic theorem. Specifically,

$$\hat{H}(t) = \hat{H}_\lambda(t) + \hat{H}_{CD}(t), \quad \hat{H}_{CD}(t) = \dot{\lambda}(t) \hat{A}_\lambda, \quad (5)$$

where the CD Hamiltonian is expressed in terms of adiabatic gauge potential (AGP),  $\hat{A}_\lambda$ , and the rate of change of the scheduling function  $\dot{\lambda}(t)$ . It is evident that when the adiabatic condition is satisfied as  $T \rightarrow \infty$ , the CD-Hamiltonian vanishes. Instead, at short times this term becomes significant, dominating the dynamics in the impulse regime [69, 70]. The AGP translates infinitesimal displacements in the parameter space into the Hilbert space, thereby canceling diabatic transitions [71]. However, determining the exact AGP is as complex as solving the original Hamiltonian. To compute the AGP for complex many-body systems, such as molecular problems where analytic solutions are unfeasible, we employ the variational CD method [48] to define  $\hat{H}_{CD}(t)$ . To do this, we write a nested commutator expansion of the Hamiltonian and its derivative with respect to  $\lambda$  [47]:

$$\hat{A}_\lambda^{(l)} = i \sum_{k=1}^l \alpha_k \underbrace{[\hat{H}_\lambda, [\hat{H}_\lambda, \dots [\hat{H}_\lambda, \partial_\lambda \hat{H}_\lambda]]]}_{2k-1}, \quad (6)$$

where  $l$  is the expansion order of the nested commutator, and  $\{\alpha_k\}$  are the free parameters to be optimized for finding the closest operator to the exact  $\hat{A}_\lambda$ . The nested commutator expansion offers an efficient [72] and systematic protocol to calculate the AGP, and ensures convergence to the complete AGP operator when  $l \rightarrow \infty$ . Typically, the parameters  $\vec{\alpha} \equiv \{\alpha_k\}$  are determined by minimizing the action [48], i.e.,

$$S_l(\vec{\alpha}) = \text{Tr}[\hat{G}_l(\vec{\alpha})^2], \quad \hat{G}_l(\vec{\alpha}) = \partial_\lambda \hat{H}_\lambda - i[\hat{H}_\lambda, \hat{A}_\lambda^{(l)}(\vec{\alpha})]. \quad (7)$$

The action  $S_l(\vec{\alpha})$  reaches the global minimum when the approximate AGP matches the exact one. Alternatively, other classical or quantum optimization techniques, such as neural networks [49, 50], genetic algorithms [73], and circuit learning [74], can be further used or combined for optimizing these parameters in scenarios where action minimization for approximate CD term is not sufficiently efficient, particularly as the system size and interaction range increase.

### III. CD-ASSISTED ADIABATIC STATE PREPARATION

In this section, we shall first investigate the molecule adiabatic state preparation in the context of AQC, which encodes the solution of a computational problem into the ground state of a time-dependent quantum Hamiltonian. In the molecule

electronic simulation, the adiabatic evolution drives the electronic molecular ground state adiabatically from the non-interacting HF state  $|\Psi_{HF}\rangle$  to the ground state of full interacting Hamiltonian (4), incorporating the non-local repulsive electron interaction. Then, this state evolution can be expressed as

$$|\Psi(t)\rangle \equiv \hat{U}(t)|\Psi_{HF}\rangle = \mathcal{T} \exp\left(-i \int_0^T \hat{H}_\lambda(t) dt\right)|\Psi_{HF}\rangle, \quad (8)$$

where  $\mathcal{T}$  denotes the time-ordering operator, ensuring the correct chronological sequence of operations during the evolution process. Here we address molecular simulation through DAQC [75]. This approach combines adiabatic and digitized computing by implementing a discretized time evolution within a circuit computational framework. The unitary evolution is approximated as:

$$\hat{U}(t) = \mathcal{T} \exp\left(-i \int_0^T \hat{H}_\lambda(t) dt\right) \approx \prod_n \prod_j \exp(-i\delta t \hat{H}_j(n\delta t)). \quad (9)$$

where  $N$  is the number of Trotter steps,  $\delta t$  is the Trotter step length, and  $\hat{H}_j$  are Pauli strings, corresponding to the Hamiltonian terms, obtained after the BK fermion-to-qubit mapping.

We introduce the CD Hamiltonian,  $\hat{H}_{CD}(t)$ , derived by the nested commutator, into the molecular Hamiltonian. Incorporating the CD Hamiltonian in the digitized circuit as the Fig. 1(b) reflects. To achieve this, we computed the first-order nested expansion of the Hamiltonian for the molecules *LiH* and *BeH<sub>2</sub>*. However, due to the complexity and length of the resulting CD Hamiltonian, which includes two-body and many-body interactions analogous to the original Hamiltonian, we do not present it explicitly here. The inclusion of  $\hat{H}_{CD}(t)$  allows us to operate within a non-adiabatic framework, effectively bridging the adiabatic and fast annealing regimes. Meanwhile, this approach reduces the time and circuit depth required for adiabatic evolution and minimizes diabatic errors associated with fast annealing in ground-state preparation. To verify this, we simulate the *LiH* and *BeH<sub>2</sub>* molecules to quantify the influence of the CD Hamiltonian on the adiabatic preparation of molecule's ground state, by comparing the energy convergence for different evolution times and Trotter step lengths, both with and without the CD terms (see Fig. 2). The CD Hamiltonian is derived from the first-order nested expansion, see Eq. 5, to maintain compact the  $H_{CD}$ . However, higher-order expansions can be further implemented for larger molecules where more precise CD Hamiltonians are required.

Figure 2(a) and (b) present the discrepancy in ground-state energy between the simulated and analytic solutions for the *LiH* and *BeH<sub>2</sub>* molecules, where the ground-state energy convergence is calculated as

$$\epsilon = E(T; \vec{R}_b) - E_0(\vec{R}_b). \quad (10)$$

Here,  $E(T; \vec{R}_b) = \langle \Psi(T; \vec{R}_b) | \hat{H}(T) | \Psi(T; \vec{R}_b) \rangle$  represents the final results obtained from digitized adiabatic simulation, which can be calculated from the Hamiltonian  $\hat{H}(t)$  in Eq. (5) with and without the CD Hamiltonian.  $E_0(\vec{R}_b)$  is the exact analytic solution calculated from diagonalization. In the numerical simulation, the molecule bond distances are chosen as

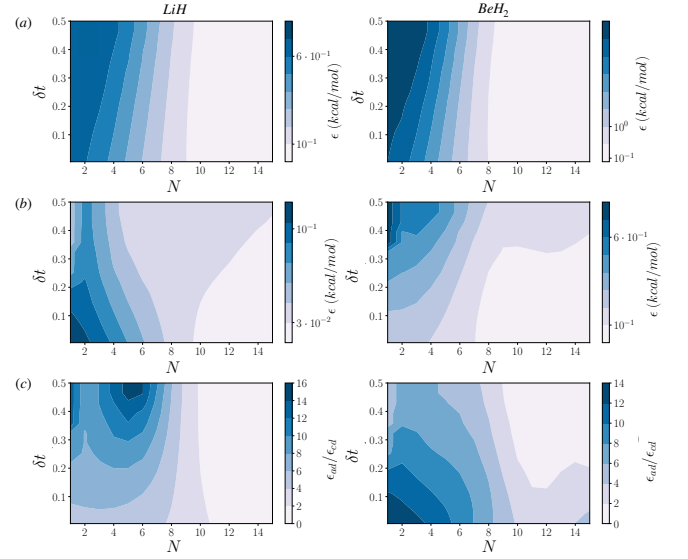


FIG. 2. Ground-state energy convergence  $\epsilon$  (see Eq. 10) and its comparison with and without the CD Hamiltonian for the molecules *LiH* (left) and *BeH<sub>2</sub>* (right) as a function of Trotter step size ( $\delta t$ ) and number of Trotter steps ( $N$ ) in atomic units. (a) and (b) present the energy convergence for the digitized adiabatic preparation with and without CD terms, improving the energy convergence below the chemical accuracy threshold. (c) compares adiabatic simulation against CD-assisted evolution, demonstrating a generalized improvement, especially for small  $\delta t$  and  $N$ .

$\vec{R}_b = 1.55\text{\AA}$  for *LiH* and  $\vec{R}_b = 1.33\text{\AA}$  for *BeH<sub>2</sub>*. A comparison between Fig. 2(a) and (b) reveals that incorporating the CD Hamiltonian increases the convergence, thus implying the speedup of adiabatic state preparation. Moreover, Fig. 2(c) illustrates the ratio between the original adiabatic and the CD-assisted evolutions, highlighting the enhancement in convergence.

Remarkably, the enhanced performance of adiabatic state preparation is demonstrated in Fig. 2(c) upon introducing the CD interactions. The overall convergence shows significant improvement across all Trotter lengths and steps, particularly at short final times  $T = \delta t N$  when the adiabatic condition is not fulfilled. During rapid evolution, the CD Hamiltonian primarily drives the state evolution, as its influence through  $\lambda(t)$  in Eq. (5) is inversely proportional to the evolution speed. As previously mentioned, in the impulse region, the CD terms become dominant. Notably, although the CD Hamiltonian increases the size of the evolving Hamiltonian (5) by approximately 2 times (incurring the cost of STA), it ultimately reduces the overall circuit depth by achieving equivalent or superior fidelity within shallower circuit depths. Furthermore, CD-assisted adiabatic evolution consistently produces results below the threshold for chemical accuracy (1 kcal/mol [76], a reference point in classical quantum chemistry).

Moreover, from Fig. 2, we analyze the influence of the CD Hamiltonian on Trotter and adiabatic errors in digitized AQC. Trotter errors arise from the discretization of continuous evolution, inducing errors of the order of  $O(\delta t^2 N \| [H_{pq}, H_{pqrs}] \|)$ , where  $H_{pq}$  and  $H_{pqrs}$  correspond to the one-electron Hamil-

tonian and the electronic Coulomb repulsion, respectively. These are the first and second terms of Eq. (2) after the BK transformation. The quadratic time step dependence of these errors causes them to increase within the  $\delta t$  axis, as shown in Fig. 2(a) for small  $N$ . Adiabatic errors, on the other hand, result from the breach of the adiabatic condition, inducing errors inversely proportional to the total evolution time  $T$ , leading to uniformly distributed errors, as evidenced in Fig. 2(a) for large  $N$ . Fig. 2(c) demonstrates that the CD Hamiltonian influences both adiabatic and Trotter errors. For the  $LiH$  molecule, it significantly reduces Trotter errors concentrated at large  $\delta t$ . On the contrary, for the  $BeH_2$  molecule, it primarily mitigates adiabatic errors at reduced times  $T$ . This improvement underscores the efficacy of the CD Hamiltonian in enhancing the overall convergence of the quantum evolution.

Motivated by the advantages demonstrated by the CD Hamiltonian in adiabatic state preparation, in what follows that we will extend the CD Hamiltonian to the VQE paradigm. The current state of gate-based computation offers significant advantages over AQC, with advanced error correction techniques and the capability to handle larger systems. Adiabatic state preparation may require a large number of gates due to the need for precise control over the adiabatic evolution and the complexity of implementing the CD Hamiltonian, such as in the simulation of the Fermi-Hubbard model [77]. However, the VQE paradigm, enhanced by CD methods, can potentially reduce the overall gate count while maintaining high accuracy, making it more feasible for scaling to larger molecules on near-term quantum devices.

#### IV. VQE WITH CD-INSPIRED ANSATZ

Next, we turn to VQE [15, 16], an extended variational quantum algorithms employed in diverse quantum computational problems such as molecule simulation or portfolio optimization. The VQE algorithm implements a quantum-parametrized circuit over an easy-to-prepare initial state ( $|\Psi_0\rangle$ ). Circuit parameters are tuned by classical optimization subroutines, transporting the initial state to the molecule target final state,  $|\Psi(\vec{\theta})\rangle$ , which is determined as

$$|\Psi(\vec{\theta})\rangle = e^{-i\hat{O}(\vec{\theta})}|\Psi_0\rangle, \quad (11)$$

with  $\hat{O}(\vec{\theta})$  being the ansatz specified later (e.g., see Appendix A). Following the Ritz principle,  $E_0 \leq \langle\Psi|\hat{H}|\Psi\rangle/\langle\Psi|\Psi\rangle$ , for all trial wave functions, the cost function for optimization is designed to find the molecule's ground state by minimizing  $\langle H_0\rangle$ , the expectation value of Hamiltonian. Here we concentrate specifically on the ground state. However, the cost function can be further modified to target excited states [78, 79], enabling a spectral analysis of the electronic structure.

As we know, the performance of VQE heavily relies on the appropriate design of the ansatz  $\hat{O}(\vec{\theta})$ . Thus, a suitable ansatz must provide sufficient expressivity to transform the initial state into the target state, while avoiding unnecessary degrees of freedom that may hinder algorithm's success by inducing circuit noises and increasing the likelihood of the appearance

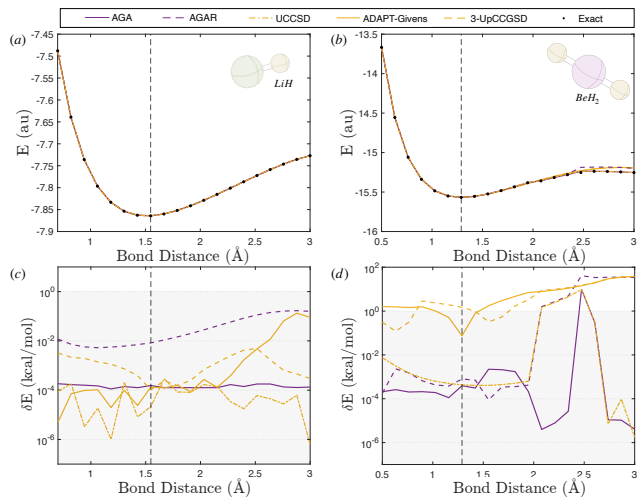


FIG. 3. VQE simulations for  $LiH$  (a),(c) and  $BeH_2$  (b),(d) molecules, where the performance of the different benchmarked ansatzes is compared with  $AGA^{(1)}$  and  $AGAR^{(1)}$ . Panels (a) and (b) depict the expected energy of ground state as a function of different bond distances. Panels (c) and (d) show the energy discrepancy between the VQE-optimized energies and the exact diagonalization results for various bond distances. The vertical dashed line marks the equilibrium bond distance, while the shaded area highlights discrepancies below the chemical accuracy threshold (1 kcal/mol).

of barren plateaus [29–31]. Inspired by the previous results on CD Hamiltonian, we design the circuit ansatz using the operator spanned by the adiabatic gauge potential. This approach, termed the AGA, uses the AGP as a template for the ansatz in VQE, shown in Fig 1(c). Based on Eq. (6), the ansatz  $\hat{O}(\vec{\theta})$  is constructed by reparametrizing each Pauli operator:

$$AGA^{(l)}(\vec{\theta}) = \sum_j \theta_j \hat{A}_j, \quad (12)$$

where  $\hat{A}_j$  are the individual Pauli string operators obtained from the nested commutators with the expansion order of  $l$ , and  $\vec{\theta} \equiv \{\theta_j\}$  are the free parameters for optimization.

The *adiabatic gauge ansatz* is a Hamiltonian variational ansatz that inherits the information contained in the CD Hamiltonian by using the adiabatic gauge potential as the CD-Hilbert space basis. As a matter of fact, the bare CD Hamiltonian  $\hat{H}_{CD}(t)$  can mimic the adiabatic evolution of the original Hamiltonian  $\hat{H}_i(t)$  up to a global phase [41]. This enables us to design AGA without requiring the complete Hamiltonian (5), thereby reducing the size and complexity. In the VQE paradigm, the reparametrization of the AGA can be efficiently determined by various classical optimizers [62], without requiring tremendous efforts for optimizing the coefficients  $\alpha_k$  in Eq. (6), see Refs. [49, 73, 74]. Furthermore, the degrees of freedom introduced by the reparametrization enhance the ansatz's expressivity, reducing the necessity for higher-order nested expansions  $l > 1$ , which in turn decreases both the computational cost and circuit depth. As mentioned earlier, for the molecules  $LiH$  and  $BeH_2$  considered, even the first-order nested expansion ( $l = 1$ ) includes two-body and many-body interactions, which can pose challenges for practical

implementation for instance in superconducting circuits [80]. Therefore, we further propose the *Reduced Adiabatic Gauge Ansatz* (AGAR), as a variant of the AGA, which is restricted to one- and two-body interactions, thereby reducing the number of gates and errors by focusing the circuit on high-fidelity operations. To evaluate the performance of the AGA against other widely used ansatzes, we will also compare it with the UCCSD [33], the 3-UpCCGSD [38], and the ADAPT-Givens VQE [35, 81] (see Appendix A). Starting from the HF initial state, i.e.,  $|\Psi_0\rangle = |\Psi_{HF}\rangle$ , we assess the ground-state energy convergence and discrepancies with respect to the exact energy for the *LiH* and *BeH<sub>2</sub>* molecules. This analysis includes studying energy convergence at various bond distances and comparing the results against the chemical accuracy threshold.

Figure 3 displays the ground state energy (a,b) and error relative (c,d) to the exact energy for the *LiH* and *BeH<sub>2</sub>* molecules at various bond distances, with errors compared against the benchmark for chemical accuracy. From Fig. 3(c) and (d), we observe that both  $AGA^{(1)}$  and  $AGAR^{(1)}$  consistently achieve convergence below the chemical accuracy threshold. The  $AGA^{(1)}$  approach frequently outperforms other methods, achieving convergence several orders of magnitude below the chemical accuracy  $\sim 1$  kcal/mol. The  $AGAR^{(1)}$  provides an interesting alternative, especially for hardware-limited quantum processors, due to its compact two-body term. While this reduction in parameter space introduces slight precision losses, the  $AGAR^{(1)}$  still maintains results below the chemical accuracy threshold.

For the *BeH<sub>2</sub>* molecule, two distinct convergence regions are observed. At bond distances below 2 Å, the UCCSD,  $AGA^{(1)}$ , and  $AGAR^{(1)}$  ansatzes achieve precision on the order of  $10^{-3}$  kcal/mol and ADAPT-Givens VQE and 3-UpCCGSD achieve precision closer to chemical accuracy. However, beyond this bond length, all ansatzes show a significant drop in precision. Although UCCSD and  $AGA^{(1)}$  remain relatively close to chemical accuracy,  $AGAR^{(1)}$ , ADAPT-Givens VQE, and 3-UpCCGSD in turn become less reliable. This decrease in accuracy is likely due to the diminished overlap between the HF initial state and the target ground state, which requires greater expressivity from the ansatz and complicates the optimization process. These findings suggest that extending VQE with the assisted AGA method to larger molecules could be a promising direction for future work.

Finally, we examine the total number of optimization parameters and number of Pauli terms in the ansatzes for the different cases. The number of parameters provides an indicator of the optimization landscape’s complexity, with a higher parameter count increasing the likelihood of encountering barren plateaus. Additionally, the size of the ansatz directly affects circuit noise and computational time. For our calculations, we use the AGA truncated to the first order ( $l = 1$ ) of the nested expansion. This choice is based on its demonstrated expressivity in reaching the system’s ground state. As shown in Table I, for the *LiH* molecule, the  $AGAR^{(1)}$  significantly reduces both the number of parameters and gates compared to other alternatives. The  $AGA^{(1)}$  thus offers a reduction in terms compared to the UCCSD ansatz. The Hamiltonian size for the

	UCCSD	AGA	AGAR	3-UpCCGSD	ADAPT-Givens
<b><i>H<sub>2</sub></i></b>	4 (14)	2	2	18	2
<b><i>LiH</i></b>	20 (130)	56	9	54	13*
<b><i>BeH<sub>2</sub></i></b>	77 (574)	30*	10*	108	10*

TABLE I. Number of parameters (terms) for the ansatzes used in VQE simulation. For bond-dependent ansatzes, the values are provided at specific bond distance,  $\bar{R}_b = 1.55\text{Å}$  for *LiH* and  $\bar{R}_b = 1.33\text{Å}$  for *BeH<sub>2</sub>*, indicated by [\*].

*BeH<sub>2</sub>* molecule is influenced by the inter-atomic distance, affecting the CD-inspired ansatz. At bond distance, both  $AGA^{(1)}$  and  $AGAR^{(1)}$  exhibit fewer parameters and terms compared to other methods. The ADAPT-Givens ansatz is also considered at different bond distances, as it pre-optimizes the ansatz pool for each specific bond distance, see Appendix A. For completeness, we also include the simple *H<sub>2</sub>* molecule in our analysis where only 2 parameters in the AGA and AGAR are sufficient.

## V. CONCLUSION AND OUTLOOK

In conclusion, we have utilized STA in molecular ground state preparation across two prominent quantum computing frameworks AQC and VQE. Our findings underscore the significant benefits STA techniques, particularly the CD driving, bring to quantum chemistry simulations, including resource reduction and enhanced convergence. First, the incorporation of CD interaction into digitized AQC enhances the convergence to the ground state, reduces evolution time, and shortens circuit depth. Also, CD terms mitigate errors from Trotterization, improving the reliability of AQC. Despite its promise, AQC may face challenges due to current quantum architecture limitations. However, its optimization-free nature will make it a viable candidate for future simulations of large molecules.

In addition, we have introduced the AGA, inspired by the adiabatic gauge potential. This ansatz effectively reduces circuit size without compromising performance, showing competitive results against other commonly used ansatzes like UCCSD and 3-UpCCGSD. To further adapt AGA to current experimental constraints, we proposed the reduced version, which simplifies the ansatz by considering only one- and two-qubit interactions. This reduction significantly lowers the number of optimization terms, demonstrating robust performance at smaller inter-atomic distances. However, AGAR’s accuracy decreases at longer distances due to its simplified nature. Overall, this work establishes a critical starting point for leveraging CD-inspired ansatz in molecular simulations and paves the way for more advanced, resource-efficient quantum chemistry methods.

With the advantages of CD driving, several promising avenues for further exploration arise. For instance, combining AGA with advanced techniques such as ADAPT-Givens VQE [35, 82] and STA Krylov space method [83, 84] could lead

to the development of hybrid ansatzes, that enhance both efficiency and accuracy in (larger) molecular simulations. In addition, one can also explore how CD driving can be adapted for calculating excited states [78, 79], facilitating a more comprehensive understanding of molecular spectra and electronic structures. Certainly, these results can be simulated or implemented on current quantum devices or cloud quantum computing platforms after appropriate decomposition and compilation. However, as quantum technology progresses, the practicality of AQC and VQE approaches, augmented with CD driving, will improve particularly with the feasibility of many-body interactions and advancements in error mitigation strategies. We hope that the simplicity of AQC and the reduced circuit complexity of AGAR are particularly promising for future NISQ devices, where engineering challenges related to many-body interactions and gate fidelities remain significant.

#### ACKNOWLEDGEMENT

This work is partially supported by the Basque Government through Grant No. IT1470-22, EU FET Open Grant EPIQUS (899368), HORIZON-CL4-2022-QUANTUM-01-SGA project 101113946 OpenSuperQ-Plus100 of the EU Flagship on Quantum Technologies,

the project grant PID2021-126273NB-I00 funded by MCIN/AEI/10.13039/501100011033, by “ERDFA way of making Europe”, “ERDF Invest in your Future”, Nanoscale NMR and complex systems (PID2021-126694NB-C21), the Spanish Ministry of Economic Affairs and Digital Transformation through the QUANTUM ENIA project call – Quantum Spain project, and the European Union through the Recovery, Transformation and Resilience Plan–NextGenerationEU within the framework of the Digital Spain 2026 Agenda. J.F.V. acknowledges support from the UPV/EHU and TECNALIA 2021 PIF contract call, from the Basque Government through the “Plan complementario de comunicación cuántica” (EXP.2022/01341) (A/20220551), from the Basque Government through the ELKARTEK program, project “KUBIT - Kuantikaren Berrikuntzarako Ikasketa Teknologikoa” (KK-2024/00105), and from the Spanish Ministry of Science and Innovation under the Recovery, Transformation and Resilience Plan (CUCO, MIG-20211005). I.I.Z. acknowledges support from UPV/EHU Ph.D. Grant No. PIF 23/246.

#### CODE AVAILABILITY

The underlying code for this study will be made available on request from the corresponding author.

- 
- [1] J. P. Dowling and G. J. Milburn, Quantum technology: the second quantum revolution, *Philosophical Transactions of the Royal Society of London. Series A: Mathematical, Physical and Engineering Sciences* **361**, 1655 (2003).
- [2] J. I. Cirac and P. Zoller, Quantum computations with cold trapped ions, *Physical review letters* **74**, 4091 (1995).
- [3] N. Gisin and R. Thew, Quantum communication, *Nature photonics* **1**, 165 (2007).
- [4] C. H. Bennett and G. Brassard, Quantum cryptography: Public key distribution and coin tossing, *Theoretical computer science* **560**, 7 (2014).
- [5] C. L. Degen, F. Reinhard, and P. Cappellaro, Quantum sensing, *Reviews of modern physics* **89**, 035002 (2017).
- [6] M. W. Doherty, N. B. Manson, P. Delaney, F. Jelezko, J. Wrachtrup, and L. C. Hollenberg, The nitrogen-vacancy colour centre in diamond, *Physics Reports* **528**, 1 (2013).
- [7] R. P. Feynman, Simulating physics with computers, international journal of theoretical physics, *International Journal of Theoretical Physics* **21**, 467 (1982).
- [8] R. A. Friesner, Ab initio quantum chemistry: Methodology and applications, *Proceedings of the National Academy of Sciences* **102**, 6648 (2005).
- [9] R. J. Bartlett and M. Musiał, Coupled-cluster theory in quantum chemistry, *Reviews of Modern Physics* **79**, 291 (2007).
- [10] A. Y. Kitaev, Quantum measurements and the abelian stabilizer problem, *arXiv preprint quant-ph/9511026* (1995).
- [11] D. S. Abrams and S. Lloyd, Quantum algorithm providing exponential speed increase for finding eigenvalues and eigenvectors, *Physical Review Letters* **83**, 5162 (1999).
- [12] A. Aspuru-Guzik, A. D. Dutoi, P. J. Love, and M. Head-Gordon, Simulated quantum computation of molecular energies, *Science* **309**, 1704 (2005).
- [13] E. Farhi, J. Goldstone, S. Gutmann, and M. Sipser, Quantum computation by adiabatic evolution, *arXiv preprint quant-ph/0011106* (2000).
- [14] P. Hauke, H. G. Katzgraber, W. Lechner, H. Nishimori, and W. D. Oliver, Perspectives of quantum annealing: Methods and implementations, *Reports on Progress in Physics* **83**, 054401 (2020).
- [15] A. Peruzzo, J. McClean, P. Shadbolt, M.-H. Yung, X.-Q. Zhou, P. J. Love, A. Aspuru-Guzik, and J. L. O’Brien, A variational eigenvalue solver on a photonic quantum processor, *Nature communications* **5**, 4213 (2014).
- [16] S. McArdle, S. Endo, A. Aspuru-Guzik, S. C. Benjamin, and X. Yuan, Quantum computational chemistry, *Reviews of Modern Physics* **92**, 015003 (2020).
- [17] J. Preskill, Quantum computing in the nisq era and beyond, *Quantum* **2**, 79 (2018).
- [18] P. W. Shor, Algorithms for quantum computation: discrete logarithms and factoring, *IEEE* , 124 (1994).
- [19] L. K. Grover, A fast quantum mechanical algorithm for database search, *Association for Computing Machinery* , 212 (1996).
- [20] K. Bharti, A. Cervera-Lierta, T. H. Kyaw, T. Haug, S. Alperin-Lea, A. Anand, M. Degroote, H. Heimonen, J. S. Kottmann, T. Menke, et al., Noisy intermediate-scale quantum algorithms, *Reviews of Modern Physics* **94**, 015004 (2022).
- [21] V. Kremenetski, C. Mejuto-Zaera, S. J. Cotton, and N. M. Tubman, Simulation of adiabatic quantum computing for molecular ground states, *The Journal of Chemical Physics* **155** (2021).
- [22] E. Granet, K. Ghanem, and H. Dreyer, Practicality of quantum adiabatic algorithm for chemistry applications, *arXiv preprint*

- arXiv:2407.09993 (2024).
- [23] A. D. King, A. Nocera, M. M. Rams, J. Dziarmaga, R. Wiersema, W. Bernoudy, J. Raymond, N. Kaushal, N. Heinsdorf, R. Harris, et al., Computational supremacy in quantum simulation, [arXiv preprint arXiv:2403.00910](#) (2024).
- [24] B. F. Schiffer, A. F. Rubio, R. Trivedi, and J. I. Cirac, The quantum adiabatic algorithm suppresses the proliferation of errors, [arXiv preprint arXiv:2404.15397](#) (2024).
- [25] P. J. J. O’Malley, R. Babbush, I. D. Kivlichan, J. Romero, McClean, et al., Scalable quantum simulation of molecular energies, *Physical Review X* **6**, 031007 (2016).
- [26] A. Kandala, A. Mezzacapo, K. Temme, M. Takita, M. Brink, J. M. Chow, and J. M. Gambetta, Hardware-efficient variational quantum eigensolver for small molecules and quantum magnets, *Nature* **549**, 242 (2017).
- [27] J. I. Colless, V. V. Ramasesh, D. Dahlen, M. S. Blok, M. E. Kimchi-Schwartz, J. R. McClean, J. Carter, W. A. de Jong, and I. Siddiqi, Computation of molecular spectra on a quantum processor with an error-resilient algorithm, *Phys. Rev. X* **8**, 011021 (2018).
- [28] S. Guo, J. Sun, H. Qian, M. Gong, Y. Zhang, F. Chen, Y. Ye, Y. Wu, S. Cao, K. Liu, et al., Experimental quantum computational chemistry with optimized unitary coupled cluster ansatz, *Nature Physics*, 1 (2024).
- [29] M. Cerezo, A. Sone, T. Volkoff, L. Cincio, and P. J. Coles, Cost function dependent barren plateaus in shallow parametrized quantum circuits, *Nature communications* **12**, 1791 (2021).
- [30] Z. Holmes, K. Sharma, M. Cerezo, and P. J. Coles, Connecting ansatz expressibility to gradient magnitudes and barren plateaus, *PRX Quantum* **3**, 010313 (2022).
- [31] M. Larocca, S. Thanasilp, S. Wang, K. Sharma, J. Bi Monte, P. J. Coles, L. Cincio, J. R. McClean, Z. Holmes, and M. Cerezo, A review of barren plateaus in variational quantum computing, [arXiv preprint arXiv:2405.00781](#) (2024).
- [32] I. G. Ryabinkin, T.-C. Yen, S. N. Genin, and A. F. Izmaylov, Qubit coupled cluster method: a systematic approach to quantum chemistry on a quantum computer, *Journal of chemical theory and computation* **14**, 6317 (2018).
- [33] A. Anand, P. Schleich, S. Alperin-Lea, P. W. Jensen, S. Sim, M. Díaz-Tinoco, J. S. Kottmann, M. Degroote, A. F. Izmaylov, and A. Aspuru-Guzik, A quantum computing view on unitary coupled cluster theory, *Chemical Society Reviews* **51**, 1659 (2022).
- [34] A. Kandala, A. Mezzacapo, K. Temme, M. Takita, M. Brink, J. M. Chow, and J. M. Gambetta, Hardware-efficient variational quantum eigensolver for small molecules and quantum magnets, *Nature* **549**, 242 (2017).
- [35] H. R. Grimsley, S. E. Economou, E. Barnes, and N. J. Mayhall, An adaptive variational algorithm for exact molecular simulations on a quantum computer, *Nature Communications* **10**, 3007 (2019).
- [36] P. K. Barkoutsos, J. F. Gonthier, I. Sokolov, N. Moll, G. Salis, A. Fuhrer, M. Ganzhorn, D. J. Egger, M. Troyer, A. Mezzacapo, et al., Quantum algorithms for electronic structure calculations: Particle-hole hamiltonian and optimized wave-function expansions, *Physical Review A* **98**, 022322 (2018).
- [37] J. R. McClean, S. Boixo, V. N. Smelyanskiy, R. Babbush, and H. Neven, Barren plateaus in quantum neural network training landscapes, *Nature Communications* **9**, 4812 (2018).
- [38] J. Lee, W. J. Huggins, M. Head-Gordon, and K. B. Whaley, Generalized unitary coupled cluster wave functions for quantum computation, *Journal of chemical theory and computation* **15**, 311 (2018).
- [39] D. Wecker, M. B. Hastings, and M. Troyer, Progress towards practical quantum variational algorithms, *Physical Review A* **92**, 042303 (2015).
- [40] D. Guéry-Odelin, A. Ruschhaupt, A. Kiely, E. Torrontegui, S. Martínez-Garaot, and J. G. Muga, Shortcuts to adiabaticity: Concepts, methods, and applications, *Reviews of Modern Physics* **91**, 045001 (2019).
- [41] M. V. Berry, Transitionless quantum driving, *Journal of Physics A: Mathematical and Theoretical* **42**, 365303 (2009).
- [42] M. Demirplak and S. A. Rice, Adiabatic population transfer with control fields, *The Journal of Physical Chemistry A* **107**, 9937 (2003).
- [43] X. Chen, I. Lizuain, A. Ruschhaupt, D. Guéry-Odelin, and J. Muga, Shortcut to adiabatic passage in two- and three-level atoms, *Physical review letters* **105**, 123003 (2010).
- [44] A. Del Campo, Shortcuts to adiabaticity by counterdiabatic driving, *Physical review letters* **111**, 100502 (2013).
- [45] S. Deffner, C. Jarzynski, and A. del Campo, Classical and quantum shortcuts to adiabaticity for scale-invariant driving, *Physical Review X* **4**, 021013 (2014).
- [46] S. Campbell, G. De Chiara, M. Paternostro, G. M. Palma, and R. Fazio, Shortcut to adiabaticity in the Lipkin-Meshkov-Glick model, *Phys. Rev. Lett.* **114**, 177206 (2015).
- [47] P. W. Claeys, M. Pandey, D. Sels, and A. Polkovnikov, Floquet-engineering counterdiabatic protocols in quantum many-body systems, *Phys. Rev. Lett.* **123**, 090602 (2019).
- [48] D. Sels and A. Polkovnikov, Minimizing irreversible losses in quantum systems by local counterdiabatic driving, *Proceedings of the National Academy of Sciences* **114** (2017).
- [49] J. Yao, L. Lin, and M. Bukov, Reinforcement learning for many-body ground-state preparation inspired by counterdiabatic driving, *Phys. Rev. X* **11**, 031070 (2021).
- [50] A. Ferrer-Sánchez, C. Flores-Garrigos, C. Hernani-Morales, J. J. Orquín-Marqués, N. N. Hegade, A. G. Cadavid, I. Montalbán, E. Solano, Y. Vives-Gilabert, and J. D. Martín-Guerrero, Physics-informed neural networks for an optimal counterdiabatic quantum computation, *Machine Learning: Science and Technology* **5**, 025035 (2024).
- [51] I. Čepaitė, A. Polkovnikov, A. J. Daley, and C. W. Duncan, Counterdiabatic optimized local driving, *PRX Quantum* **4**, 010312 (2023).
- [52] N. N. Hegade, K. Paul, Y. Ding, M. Sanz, F. Albarrán-Arriagada, E. Solano, and X. Chen, Shortcuts to adiabaticity in digitized adiabatic quantum computing, *Physical Review Applied* **15**, 024038 (2021).
- [53] H. Zhou, Y. Ji, X. Nie, X. Yang, X. Chen, J. Bian, and X. Peng, Experimental realization of shortcuts to adiabaticity in a nonintegrable spin chain by local counterdiabatic driving, *Phys. Rev. Appl.* **13**, 044059 (2020).
- [54] G. Passarelli, V. Cataudella, R. Fazio, and P. Lucignano, Counterdiabatic driving in the quantum annealing of the  $p$ -spin model: A variational approach, *Phys. Rev. Res.* **2**, 013283 (2020).
- [55] C. Mc Keever and M. Lubasch, Towards adiabatic quantum computing using compressed quantum circuits, *PRX Quantum* **5**, 020362 (2024).
- [56] K. Takahashi, Shortcuts to adiabaticity for quantum annealing, *Physical Review A* **95**, 012309 (2017).
- [57] K. Takahashi, Hamiltonian engineering for adiabatic quantum computation: Lessons from shortcuts to adiabaticity, *Journal of the Physical Society of Japan* **88**, 061002 (2019).
- [58] A. Hartmann and W. Lechner, Rapid counter-diabatic sweeps in lattice gauge adiabatic quantum computing, *New Journal of Physics* **21**, 043025 (2019).

- [59] L. Prielinger, A. Hartmann, Y. Yamashiro, K. Nishimura, W. Lechner, and H. Nishimori, Two-parameter counter-diabatic driving in quantum annealing, *Phys. Rev. Res.* **3**, 013227 (2021).
- [60] J. Wurtz and P. J. Love, Counterdiabaticity and the quantum approximate optimization algorithm, *Quantum* **6**, 635 (2022).
- [61] P. Chandarana, N. N. Hegade, K. Paul, F. Albarrán-Arriagada, E. Solano, A. Del Campo, and X. Chen, Digitized-counterdiabatic quantum approximate optimization algorithm, *Physical Review Research* **4**, 013141 (2022).
- [62] R. Xu, J. Tang, P. Chandarana, K. Paul, X. Xu, M. Yung, and X. Chen, Benchmarking hybrid digitized-counterdiabatic quantum optimization, *Phys. Rev. Res.* **6**, 013147 (2024).
- [63] Z. Zhan, C. Run, Z. Zong, L. Xiang, Y. Fei, Z. Sun, Y. Wu, Z. Jia, P. Duan, J. Wu, Y. Yin, and G. Guo, Experimental determination of electronic states via digitized shortcut to adiabaticity and sequential digitized adiabaticity, *Phys. Rev. Appl.* **16**, 034050 (2021).
- [64] A. Szabo and N. S. Ostlund, Modern quantum chemistry: introduction to advanced electronic structure theory, Courier Corporation (2012).
- [65] J. R. McClean, N. C. Rubin, K. J. Sung, I. D. Kivlichan, X. Bonet-Monroig, et al., Openfermion: the electronic structure package for quantum computers, *Quantum Science and Technology* **5**, 034014 (2020).
- [66] P. Jordan and E. Wigner, Über das paulische äquivalenzverbot, *Zeitschrift für Physik* **47**, 631 (1928).
- [67] S. B. Bravyi and A. Y. Kitaev, Fermionic quantum computation, *Annals of Physics* **298**, 210 (2002).
- [68] J. T. Seeley, M. J. Richard, and P. J. Love, The bravyi-kitaev transformation for quantum computation of electronic structure, *The Journal of Chemical Physics* **137** (2012).
- [69] P. Chandarana, N. N. Hegade, I. Montalban, E. Solano, and X. Chen, Digitized counterdiabatic quantum algorithm for protein folding, *Phys. Rev. Appl.* **20**, 014024 (2023).
- [70] A. G. Cadavid, I. Montalban, A. Dalal, E. Solano, and N. N. Hegade, Efficient dcqo algorithm within the impulse regime for portfolio optimization, arXiv preprint arXiv:2308.15475 (2023).
- [71] C. Jarzynski, Generating shortcuts to adiabaticity in quantum and classical dynamics, *Phys. Rev. A* **88**, 040101 (2013).
- [72] A. M. Childs, Y. Su, M. C. Tran, N. Wiebe, and S. Zhu, Theory of trotter error with commutator scaling, *Phys. Rev. X* **11**, 011020 (2021).
- [73] P. R. Hegde, G. Passarelli, A. Scocco, and P. Lucignano, Genetic optimization of quantum annealing, *Phys. Rev. A* **105**, 012612 (2022).
- [74] D. Sun, P. Chandarana, Z.-H. Xin, and X. Chen, Optimizing counterdiabaticity by variational quantum circuits, *Philosophical Transactions of the Royal Society A: Mathematical, Physical and Engineering Sciences* **380**, 20210282 (2022).
- [75] R. Barends, A. Shabani, L. Lamata, J. Kelly, A. Mezzacapo, U. L. Heras, R. Babbush, A. G. Fowler, B. Campbell, Y. Chen, et al., Digitized adiabatic quantum computing with a superconducting circuit, *Nature* **534**, 222 (2016).
- [76] The chemical accuracy is defined from the common errors committed in thermodynamic experiments ( $\sim 1\text{kcal/mol}$ ).
- [77] J. Tang, R. Xu, Y. Ding, X. Xu, Y. Ban, M. Yung, A. Pérez-Obiol, G. Platero, and X. Chen, Exploring ground states of fermi-hubbard model on honeycomb lattices with counterdiabaticity, arXiv preprint arXiv:2405.09225 (2024).
- [78] O. Higgott, D. Wang, and S. Brierley, Variational quantum computation of excited states, *Quantum* **3**, 156 (2019).
- [79] K. M. Nakanishi, K. Mitarai, and K. Fujii, Subspace-search variational quantum eigensolver for excited states, *Phys. Rev. Res.* **1**, 033062 (2019).
- [80] R. Barends, A. Shabani, L. Lamata, J. Kelly, A. Mezzacapo, et al., Digitized adiabatic quantum computing with a superconducting circuit, *Nature* **534**, 222 (2016).
- [81] J. M. Arrazola, O. Di Matteo, N. Quesada, S. Jahangiri, A. Delgado, and N. Killoran, Universal quantum circuits for quantum chemistry, *Quantum* **6**, 742 (2022).
- [82] L. Zhu, H. L. Tang, G. S. Barron, F. A. Calderon-Vargas, N. J. Mayhall, E. Barnes, and S. E. Economou, Adaptive quantum approximate optimization algorithm for solving combinatorial problems on a quantum computer, *Phys. Rev. Res.* **4**, 033029 (2022).
- [83] K. Takahashi and A. del Campo, Shortcuts to adiabaticity in krylov space, *Physical Review X* **14** (2024).
- [84] B. Bhattacharjee, A lanczos approach to the adiabatic gauge potential, arXiv preprint quant-ph/9511026 (2023).
- [85] V. Bergholm, J. Izaac, M. Schuld, C. Gogolin, S. Ahmed, V. Ajith, M. S. Alam, G. Alonso-Linaje, B. Akash-Narayanan, A. Asadi, et al., Pennylane: Automatic differentiation of hybrid quantum-classical computations, arXiv preprint arXiv:1811.04968 (2018).

## Appendix A: Different ansatzes for VQE

In this Appendix, we briefly introduce the ansatzes used in our paper for the sake of clarity. Here 3-UpCCGSD and ADAPT-Givens VQE are simulated using PennyLane packages [81, 85].

**UCCSD.**– The Unitary Coupled Cluster with Single and Double excitations (UCCSD) ansatz is a unitary extension of the Coupled Cluster (CC) method, truncated at the second order of expansion. The CC ansatz is defined by a sum of excitation operators, as specified in Eqs. (A1) and (A2). To achieve unitarity, these excitation operators are expressed in terms of their anti-Hermitian sum. The excitation operators are given by:

$$\hat{T}_1 = \sum_{i,a} t_i^a \hat{a}_a^\dagger \hat{a}_i, \quad (\text{A1})$$

$$\hat{T}_2 = \frac{1}{4} \sum_{i,j,a,b} t_{ij}^{ab} \hat{a}_a^\dagger \hat{a}_b^\dagger \hat{a}_i \hat{a}_j, \quad (\text{A2})$$

where  $\hat{a}^\dagger$  and  $\hat{a}$  are annihilation and creation fermionic operators, respectively, and  $t_{ij}^{ab}$ ,  $t_i^a$  are the optimization parameters. The index  $a, b, c, d, \dots$  refer to unoccupied orbitals, while  $i, j, k, l, \dots$  denote occupied orbitals. The unitary operator for the UCCSD ansatz is defined as:

$$\hat{U}(\vec{\theta}) = e^{\hat{T}(\vec{\theta}) - \hat{T}(\vec{\theta})^\dagger}, \quad (\text{A3})$$

where  $\vec{\theta}$  represents parameters for optimization in the VQE algorithm.

**k-Unitary Pair Coupled Cluster Generalized Singles and Doubles (k-UpCCGSD).**– The k-UpCCGSD ansatz is a variant within the CC family, designed to reduce the operator pool by focusing on a subset of excitation operators. It restricts the terms to paired double excitations and generalized singles. Generalized singles do not distinguish between

occupied and unoccupied orbitals, while paired doubles exclusively move paired electrons between spatial orbitals. The pair double and generalized single operators are defined as:

$$\hat{T}_1 = \sum_{pq} t_p^q \hat{a}_p^\dagger \hat{a}_q, \quad (\text{A4})$$

$$\hat{T}_2 = \sum_{ia} t_{ia}^{a\alpha} \hat{a}_{i\alpha}^\dagger \hat{a}_a^\dagger \hat{a}_\alpha \hat{a}_{i\alpha}, \quad (\text{A5})$$

where  $t_p^q$  and  $t_{ia}^{a\alpha}$  are the optimization parameters for the generalized singles and paired doubles, respectively and  $p, q, r, s, \dots$  represent both type of orbital occupied or unoccupied. In a word, the circuit unitary operator for the k-UpCCGSD ansatz is given by:

$$\hat{U}(\theta) = \prod_{j=1}^k e^{\hat{T}(\vec{\theta}) - \hat{T}(\vec{\theta})^\dagger}, \quad (\text{A6})$$

where  $k = 3$  denotes the number of times the UpCCGSD is applied.

**ADAPT-VQE.**— ADAPT-VQE is not a specific ansatz but rather a variational protocol used to optimize the ansatz by selecting the most influential terms from a larger pool. This protocol incrementally builds the ansatz by identifying and including operators that contribute significantly to the gradient

of the expected energy. For the step  $n$ , ADAPT-VQE evaluates the gradient of the expected energy with respect to each operator coefficient as given by:

$$\frac{\partial E^{(n)}}{\partial \theta_k} = \langle \Psi^{(n)} | [\hat{H}, \hat{A}_k] | \Psi^{(n)} \rangle. \quad (\text{A7})$$

Here,  $\langle \Psi^{(n)} | [\hat{H}, \hat{A}_k] | \Psi^{(n)} \rangle$  represents the commutator of the Hamiltonian  $\hat{H}$  with the operator  $\hat{A}_k$ , and  $\theta_k$  is the parameter associated with  $\hat{A}_k$ . The protocol continues to add operators to the ansatz until the norm of the gradient falls below a pre-determined threshold  $\epsilon$ .

In our study, the ADPAT-VQE protocol is implemented using the Givens rotations (GR) protocol. GRs are particle-conserving unitaries that operate within a restricted subspace of the larger Hilbert space. For instance, in the single excitation subspace, a GR acts on a two-dimensional subspace of the four-dimensional space of two qubits. The action of a GR on basis states is described by:

$$\begin{aligned} U|01\rangle &\rightarrow a|01\rangle + b|10\rangle, \\ U|10\rangle &\rightarrow c|01\rangle + d|10\rangle, \end{aligned}$$

where  $a, b, c, d$  are parameters defining the rotation. GRs are efficient in terms of the number of optimization parameters. However, this efficiency is balanced by the introduction of multi-qubit gates, which can be challenging to implement on current hardware due to their complexity.